blood®
Regular Article

RED CELLS, IRON, AND ERYTHROPOIESIS

CME Article

Silent infarcts in sickle cell disease occur in the border zone region and are associated with low cerebral blood flow

Andria L. Ford,[1] Dustin K. Ragan,[1] Slim Fellah,[1] Michael M. Binkley,[1] Melanie E. Fields,[2] Kristin P. Guilliams,[1,2] Hongyu An,[3] Lori C. Jordan,[4] Robert C. McKinstry,[3] Jin-Moo Lee,[1,3] and Michael R. DeBaun[4]

[1]Department of Neurology, [2]Department of Pediatrics, and [3]Mallinckrodt Institute of Radiology, Washington University School of Medicine, St. Louis, MO; and [4]Department of Pediatrics, Vanderbilt University, Nashville, TN

KEY POINTS

- The SCI density map revealed key SCI locations in the deep white matter of the frontal and parietal lobes.
- Peak SCI density occurs in the region of nadir cerebral blood flow.

Silent cerebral infarcts (SCIs) are associated with cognitive impairment in sickle cell anemia (SCA). SCI risk factors include low hemoglobin and elevated systolic blood pressure; however, mechanisms underlying their development are unclear. Using the largest prospective study evaluating SCIs in pediatric SCA, we identified brain regions with increased SCI density. We tested the hypothesis that infarct density is greatest within regions in which cerebral blood flow is lowest, further restricting cerebral oxygen delivery in the setting of chronic anemia. Neuroradiology and neurology committees reached a consensus of SCIs in 286 children in the Silent Infarct Transfusion (SIT) Trial. Each infarct was outlined and coregistered to a brain atlas to create an infarct density map. To evaluate cerebral blood flow as a function of infarct density, pseudocontinuous arterial spin labeling was performed in an independent pediatric SCA cohort. Blood flow maps were aligned to the SIT Trial infarct density map. Mean blood flow within low, moderate, and high infarct density regions from the SIT Trial were compared. Logistic regression evaluated clinical and imaging predictors of overt stroke at 3-year follow-up. The SIT Trial infarct density map revealed increased SCI density in the deep white matter of the frontal and parietal lobes. A relatively small region, measuring 5.6% of brain volume, encompassed SCIs from 90% of children. Cerebral blood flow was lowest in the region of highest infarct density ($P < .001$). Baseline infarct volume and reticulocyte count predicted overt stroke. In pediatric SCA, SCIs are symmetrically located in the deep white matter where minimum cerebral blood flow occurs. (*Blood*. 2018;132(16):1714-1723)

JOINTLY ACCREDITED PROVIDER™
INTERPROFESSIONAL CONTINUING EDUCATION

Medscape Continuing Medical Education online

In support of improving patient care, this activity has been planned and implemented by Medscape, LLC and the American Society of Hematology. Medscape, LLC is jointly accredited by the Accreditation Council for Continuing Medical Education (ACCME), the Accreditation Council for Pharmacy Education (ACPE), and the American Nurses Credentialing Center (ANCC), to provide continuing education for the healthcare team.

Medscape, LLC designates this Journal-based CME activity for a maximum of 1.00 *AMA PRA Category 1 Credit(s)*™. Physicians should claim only the credit commensurate with the extent of their participation in the activity.

All other clinicians completing this activity will be issued a certificate of participation. To participate in this journal CME activity: (1) review the learning objectives and author disclosures; (2) study the education content; (3) take the post-test with a 75% minimum passing score and complete the evaluation at http://www.medscape.org/journal/blood; and (4) view/print the certificate. For the CME questions, see page 1727.

Disclosures

CME questions author Laurie Barclay, freelance writer and reviewer, Medscape, LLC, owns stock, stock options, or bonds from Pfizer. Associate Editor Mario Cazzola and the authors declare no competing financial interests.

Learning objectives

Upon completion of this activity, participants will be able to:

1. Identity the brain regions with increased silent cerebral infarct (SCI) density in children with sickle cell anemia (SCA) and their association with cerebral blood flow (CBF), according to a large prospective study
2. Explain the imaging and clinical predictors of overt stroke or recurrent silent infarct in children with SCA, according to a large prospective study
3. Determine the clinical implications of these findings regarding brain regions with increased SCI density in children with SCA and their association with CBF, according to a large prospective study

Release date: October 18, 2018; Expiration date: October 18, 2019

Introduction

Children with sickle cell anemia (SCA) are at ongoing risk for multiorgan ischemia, including a high prevalence of silent cerebral infarcts (SCIs). SCIs appear in infancy and accumulate occultly, occurring in up to 37% of children by age 14 years,[1,2] and in 53% of adults by age 32 years.[3] Beyond structural brain injury, the presence of SCIs heralds an increased risk for overt stroke,[4] failure to meet academic milestones,[5] and increased cognitive impairment when compared to children with SCA who do not have SCIs.[6-8] Mechanisms underlying SCIs in children with SCA are unclear; however, studies have identified several risk factors, including impairment in cerebral oxygen delivery resulting from low baseline hemoglobin levels[9] and acute anemic events,[10-12] as well as factors associated with injury to the cerebral vasculature, such as high blood pressure or intracranial and extracranial stenosis.[9,11,13,14]

Prior evidence suggests a spatial predilection for SCIs to occur in the white matter of the frontal and parietal lobes.[4] Further morphometry[15] and diffusion tensor imaging[16] studies have demonstrated white matter volume loss and disrupted white matter integrity, respectively. Infarct patterns including both border zone[15,17] and cortical, wedge-like infarcts[18] have been noted. Border zone infarcts indicate that global reduction in arterial oxygen content, cerebral hemodynamic factors, or both may be driving ischemic mechanisms, whereas wedge-like infarcts suggest that thromboembolic factors predominate.

As a planned secondary analysis from a multicenter randomized clinical trial in children with SCA, we tested the primary hypothesis that SCIs are commonly located in the internal border zone regions (anterior and posterior) because of ischemic vulnerability. As a secondary hypothesis, we tested the premise that the location of SCIs would overlap with regions of lowest resting cerebral blood flow. Evidence in support of our hypotheses would provide insight into the pathophysiology of SCIs in children with SCA and facilitate targeted strategies for primary and secondary prevention of cerebral infarcts.

Methods

SIT Trial design and participants

SIT Trial was a multicenter, international, randomized clinical trial in which children with SCA and SCIs received standard care (no hydroxyurea 3 months before randomization) or regular blood transfusion therapy (NCT00072761).[1] The trial was approved by the institutional review board at each of 29 participating institutions. Participants were recruited from December 2004 until May 2010. Children aged 5 to 15 years with confirmed hemoglobin SS or hemoglobin $S\beta^0$ thalassemia, and at least 1 infarct-like lesion on screening magnetic resonance imaging (MRI), scan were included. An infarct-like lesion was defined as an MRI signal abnormality at least 3 mm in 1 dimension and visible in 2 planes on fluid-attenuated inversion recovery (FLAIR) T2-weighted images, as determined by agreement of 2 of the 3 study neuroradiologists.[19] The neurology committee adjudicated a lesion as a SCI if the participant had either a normal neurologic examination or an abnormality on examination that could not be explained by the lesion location. Children were excluded if they had a history of a focal neurologic deficit associated with an infarct or hemorrhagic stroke on brain MRI, seizure disorder, treatment with hydroxyurea in the previous 3 months, history of regular transfusion therapy, or transcranial Doppler (TCD) velocities of at least 200 cm/s using the nonimaging technique, or at least 185 cm/s using an imaging technique.

Of 1074 children with SCA undergoing a screening MRI, 379 (35%) had infarct-like lesions adjudicated by the neuroradiology committee. Of these children, 96 were unable to continue participation in the randomized SIT Trial because of children and families who declined or withdrew participation, could not commit to the study timeline or had financial constraints, relocated, had overt strokes, or failed further screening criteria, leaving 289 participants for inclusion in the SIT infarct density map (Figure 1). Of this group, 196 were randomly assigned to transfusion vs observational management within the SIT clinical trial.

Image and statistical analyses

Before the start of the SIT Trial, a lesion density analysis of all MRIs was planned. The neuroradiology infarct adjudication process facilitated the planned analysis. Participants who had infarct-like lesions adjudicated by the SIT Trial neuroradiology committee were eligible for inclusion in the current study evaluating SCI location and density in pediatric SCA. The precise location and maximal diameter of each SCI adjudicated by the neuroradiology committee was recorded at the time of adjudication. T1 and FLAIR maps were skull-stripped. T1 maps were segmented into gray and white matter, using publicly available tools (FMRIB Software Library).[20,21] Lesions were manually outlined in the native FLAIR space by a board-certified vascular neurologist (A.L.F.), using publicly available software (Medical Image Processing, Analysis, and Visualization; https://mipav.cit.nih.gov/).[22] Each SCI, as previously recorded during the neuroradiologist's central adjudication, was matched to the individual's FLAIR map before manually outlining. After all SCIs within an individual were outlined, a FLAIR lesion mask for that individual was created. Individual T1 maps and corresponding

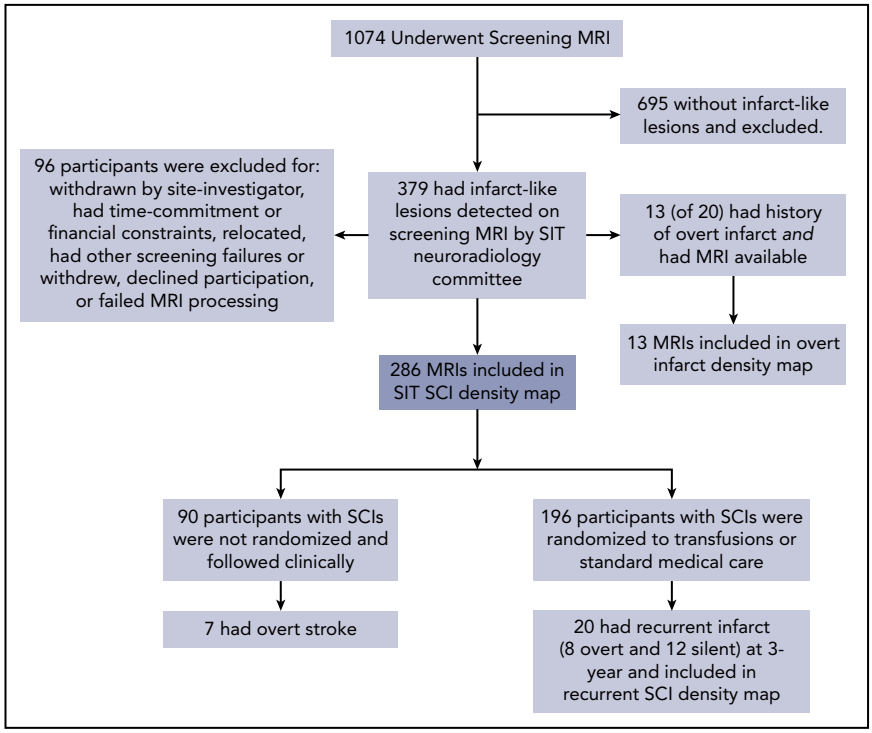

Figure 1. Participant screening and enrollment in the SIT Trial. Four density maps were created: (1) 286 children with SCA and no history of stroke who had SCIs adjudicated by the SIT neuroradiology committee after screening MRI; (2) 13 children with SCA and overt infarct who were excluded from the cohort of adjudicated SCIs; (3) baseline MRI; and (4) 3-year follow-up MRI from 20 children with SCA and no history of stroke who had SCIs adjudicated and who had recurrent overt or silent infarct by 3-year follow-up.

FLAIR lesion masks were coregistered to a common brain template (Montreal Neurological Institute),[23] using nonlinear registration[24] and placing all lesions into a common space for creation of the infarct density map. Infarct density was calculated in each voxel as the sum of participants, with a lesion in that voxel divided by the total number of participants in the cohort. The infarct density map was completed before performing the cerebral blood flow analysis described here. To determine the spatial extent of brain tissue encompassing SCIs from the majority of the cohort, the infarct density map was thresholded to include SCIs from 90% of the cohort, a threshold that was chosen before creation of the infarct density map. The volume contributing to this 90% lesion mask was calculated. To evaluate spatial symmetry of the infarct density map, voxel densities in the left hemisphere were plotted against mirror voxel densities in the right hemisphere, with number of voxels represented in the in-plane color axis. Correlation of right-left densities was calculated using Pearson's *r*. T1 images were segmented to classify gray and white matter, using FMRIB's automated segmentation tool, allowing quantification of tissue-type volumes.[25] The International Consortium for Brain Mapping lobular atlas[26] allowed classifying SCIs within anatomical lobes. Infarct volumes were reported as median (interquartile range [IQR], 25th-75th percentile). Three additional infarct density maps were created for screening MRI scans in nonrandomized SIT Trial participants who had overt infarcts (these participants were not included in the main SCI density map described here, or in the logistic regression models described next), the baseline scan of randomized children in the SIT Trial who had recurrent silent or overt infarct by 3-year follow-up, and the 3-year follow-up scan of randomized children in SIT who had overt infarct or recurrent SCIs.

Cerebral blood flow analysis

To evaluate the relationship of infarct location to resting cerebral hemodynamics, cerebral blood flow from an independent cohort of children with SCA (n = 41) was measured as a function of infarct density from the SIT Trial SCI cohort (n = 286). For the cerebral blood flow analysis, data from a prospective, observational MRI study evaluating cerebral hemodynamics in pediatric SCA was used. Enrollment criteria included children aged 5 to 21 years, laboratory-confirmed hemoglobin SS or hemoglobin Sβ^0 thalassemia, and legal guardians providing written consent. Children with overt strokes, elevated TCD velocities, prior regular transfusion therapy, stem cell transplant, or other neurologic disorder were excluded. As children with SCIs were allowed in the cerebral blood flow analysis, infarct lesions were manually delineated, using the same procedure as described for the lesion density maps, and lesion voxels were excluded from all blood flow analyses. All participants underwent a brain MRI with a Siemens 3T Tim Trio (Erlangen, Germany) with a 12-channel head coil without sedation. Cerebral blood flow was measured using a pseudocontinuous arterial spin labeling sequence (echo time/repetition time = 12/3280 milliseconds; in-plane voxel resolution = 3 × 3 mm; slice thickness = 5 mm, 22 slices; number of averages = 80; postlabel delay = 1000 milliseconds).[27] For cerebral blood flow quantification, blood T1 in the superior sagittal sinus was individually measured using an inversion-recovery echo planar imaging sequence, given its dependence on hematocrit.[28-30]

To test the hypothesis that border zone regions would demonstrate the highest infarct density within vulnerable, low-flow regions, cerebral blood flow maps from an independent pediatric SCA cohort were coregistered to the infarct density map of the SIT Trial participants so that cerebral blood flow could be measured as a function of infarct density. Before knowledge of the cerebral blood flow results, the maximal infarct density from the infarct density map was divided by 3 to allow creation of 3 equal infarct density tiers in which cerebral blood flow would be measured. Maximal infarct density was 18%; thus, the tiers

Table 1. Clinical characteristics in SIT Trial participants and an independent cohort of children with sickle cell anemia

	SIT Trial participants			Independent SCA cohort for cerebral blood flow analysis (n = 41)
	Silent cerebral infarcts (n = 286)	Overt infarct (n = 13)*	Silent cerebral infarcts with recurrent silent or overt infarct at 3-y follow-up (n = 20)†	
Age, y	9.3 (2.5)	8.5 (2.4)	8.0 (2.0)	10.8 (3.9)
Sex, male	128 (44%)	5 (38%)	12 (60%)	21 (51%)
Race, African	281 (98%)	13 (100%)	20 (100%)	41 (100%)
Hemoglobin, g/dL	8.0 (1.0)	7.7 (0.9)	7.9 (1.1)	8.5 (1.2)
Hemoglobin, F %	11 (9)	9 (4)	13 (8)	18 (10)
Hemoglobin, S %	84 (11)	81 (21)	84 (8)	76 (11)
White blood cell count $\times 10^6/\mu L$	13.2 (7.8)	10.2 (4.3)	13.7 (4.9)	10.0 (2.6)
Reticulocyte, %	12.8 (5.6)	13.2 (4.6)	13.7 (5.9)	—
$SpO_{2\%}$	96.1 (3.0)	96.3 (2.4)	96.5 (2.5)	96.7 (2.7)
Systolic BP, mm Hg	109 (11)	108 (11)	106 (12)	—

The table shows clinical characteristics of SIT Trial participants with (1) silent cerebral infarcts detected on screening, (2) overt infarcts detected on screening and not randomly allocated, and (3) silent cerebral infarcts detected on screening who were followed prospectively and subsequently developed recurrent silent cerebral infarcts or strokes. Clinical characteristics of an independent cohort of children with sickle cell anemia, including those with and without silent cerebral infarcts and who had cerebral blood flow assessment (non-SIT Trial participants), are also shown.

Data shown as mean (standard deviation) for continuous variables and N (%) for dichotomous variable.

F, fetal; S, sickle.

*SIT Trial participants, screened only (not enrolled in the trial), followed prospectively and determined to have strokes.

†SIT Trial participants enrolled in the randomized control trial.

were low infarct density (1%-6%), moderate infarct density (7%-12%), and high infarct density (13%-18%) regions. Across the 3 regions, mean white matter cerebral blood flow from the independent pediatric SCA cohort was statistically compared. The analysis was restricted to white matter because SCI densities were highest within white matter and as a result of intrinsically large differences between gray and white matter cerebral blood flow. Statistical analysis evaluated differences in cerebral blood flow across the 3 regions, using Friedman's test to account for repeated measures with pairwise comparisons using Wilcoxon signed-rank test, and adjustment for multiple testing using Benjamini-Hochberg procedure to maintain a family-wise error rate of 0.05. Similar to SCIs, an overt infarct analysis evaluated resting cerebral blood flow within regions of low (1%-25%) and high (26%-50%) infarct density. Only 2 cerebral blood flow tiers were used because of the small cohort size and range of potential infarct densities. Statistical analysis evaluated differences in cerebral blood flow across the 2 regions of overt infarct density, using Wilcoxon signed-rank test with $P < .05$ required for significance.

Logistic regression models for prediction of overt stroke and recurrent silent infarcts

To evaluate imaging and clinical predictors of overt stroke and silent infarct in children with SCA and SCIs, 2 logistic regression models were performed. In the first model, the larger SIT Trial cohort, including randomly and nonrandomly allocated participants (n = 286), was evaluated for prediction of incident overt stroke only. Recurrent SCIs could not be included in the end point for the larger cohort, as the nonrandomized children did not get 3-year follow-up imaging unless they developed neurological symptoms. For capture of overt stroke, SIT Trial project coordinators visited each site and collected follow-up data including clinic, hospital, and radiology records on all participants. A SIT Trial stroke neurologist (L.C.J.) and the principal investigator, a hematologist (M.R.D.), reviewed all source documents for suspected neurological events and independently adjudicated the presence of a new stroke. The final diagnosis for each clinical neurological event was based on review of the medical chart and brain MRI. Recurrent silent infarction had to meet imaging criteria for new silent infarction on follow-up MRI or enlargement of previous SCI by a linear increase in diameter of 3 mm or more.

In the second logistic regression model, randomly allocated participants (n = 196) with SCIs and normal TCD velocities were evaluated for infarct prediction. In this model, both incident overt stroke and recurrent SCI were included in the end point, as all participants underwent a 3-year follow-up MRI scan.

Imaging variables in the logistic regression analyses included baseline FLAIR lesion volume (defined as FLAIR lesion volume/T1 brain volume to adjust for change in brain volume with age), ratio of gray matter to white matter FLAIR lesion volume, and percentage of FLAIR lesion volume within the SIT Trial heat map region including SCIs from 90% of children. Clinical variables demonstrating significance in the SIT Trial were included as covariates: age, steady-state reticulocyte count, and parental report of recurrent headaches.[1] In addition, randomization to

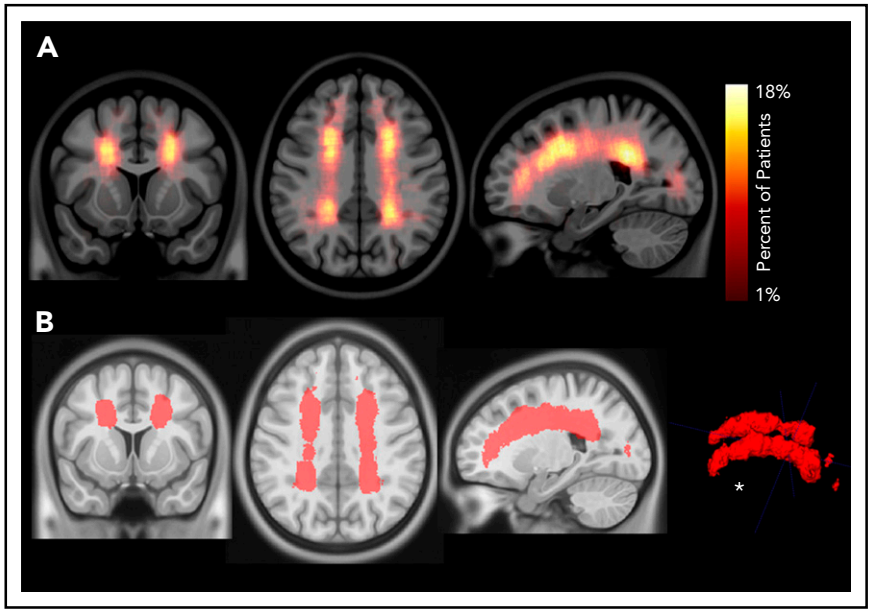

Figure 2. Infarct density map from 286 children with SCA and SCIs in the SIT Trial. Infarct density was calculated for each voxel as the sum of participants with a lesion in that voxel divided by the total number of participants evaluated in the cohort. (A) Infarct densities range from 1% to 18%, with greatest densities falling in the deep white matter of the frontal and parietal lobes. (B) The infarct density map was thresholded to determine the region which encompassed SCIs from 90% of the cohort. The volume of this region was 5.6% of total intracranial volume. *SCIs for 90% of children are located within a confined region (5.6% of total brain volume).

observational care vs regular transfusions was included as a clinical variable in the second logistic regression model predicting overt stroke and recurrent silent infarct in the participants in the subgroup who were randomly assigned in the SIT Trial (n = 196). A 2-step procedure was used for logistic regression. The first step included imaging and clinical variables, as described earlier, followed by the second step, which required a significance level of 0.1 to allow a variable into the model. *P* values were estimated with the use of a permutation test. Odds ratios are presented with the 95% likelihood ratio confidence interval.

Results

Of children screened for participation in the SIT Trial, 289 children with SCIs (and without any overt stroke history and with normal TCD measurements) had FLAIR maps available for infarct delineation. Three participants were excluded (absence of T1-weighted image in 1; inability to align the T1 to the atlas in 2), leaving 286 participants available for inclusion in the SCI density map. Baseline clinical characteristics are shown in Table 1.

Silent cerebral infarcts fall within a small, symmetric brain region in the deep white matter of the frontal and parietal lobes

To evaluate the interaction between location and frequency of SCIs in pediatric SCA, an infarct density map from 286 participants with SCIs was created (Figure 2A). Infarct frequency within voxels ranged from 1 to 51 participants, and corresponding infarct density ranged from 1 to 18%. Infarct

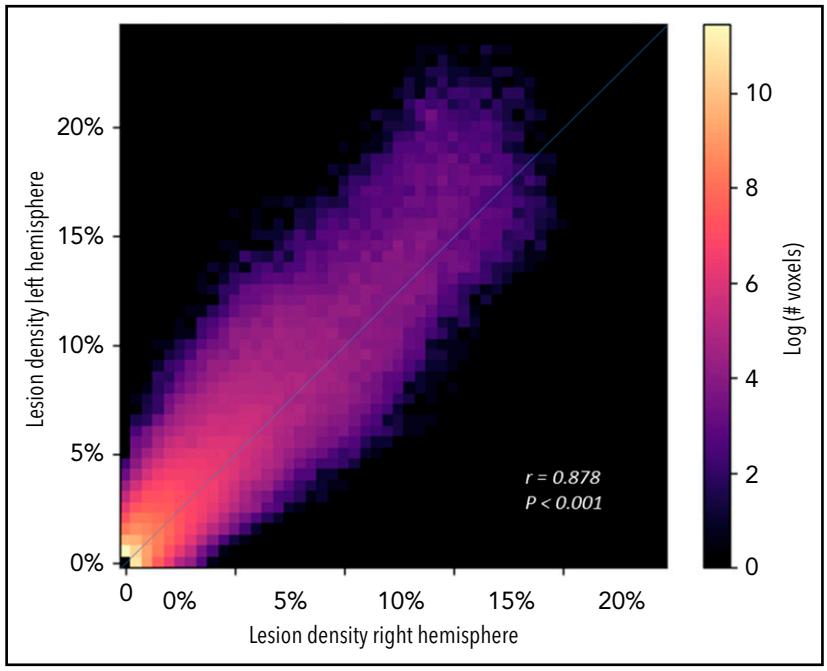

Figure 3. SCIs in pediatric SCA are symmetric. Voxel densities in the right hemisphere were plotted against mirror densities in the left hemisphere with number of voxels represented in the in-plane color axis. Correlation of right-left densities, calculated using Pearson's *r*, demonstrates high symmetry of lesion density between the 2 hemispheres.

Table 2. Tissue-type and lobar characteristics for silent cerebral infarcts in the SIT Cohort (n = 286)

SCI characteristics	
Lesion volume, mm³	
Total	381 (177, 1014)
Gray matter	33 (3, 146)
White matter	278 (125, 772)
Number (%) of patients with SCIs	
Frontal lobe	258 (90%)
Parietal lobe	152 (53%)
Temporal lobe	99 (34%)
Occipital lobe	35 (12%)
Cerebellum	4 (1%)

Volumes are shown as median (25th percentile, 75th percentile).

locations with the highest density were found in the white matter of the frontal and parietal lobes above and adjacent to the lateral ventricles.

To evaluate the spatial extent of SCIs encompassing most of the cohort, the infarct density map was thresholded to delineate the region capturing lesions from 90% of the population. SCIs from 90% of children were confined to a relatively small brain region measuring 5.6% of total brain volume (Figure 2B). The infarct density map was further analyzed for degree of symmetry between right and left hemispheres. Infarct densities for mirror voxels between the right and left hemispheres were highly symmetric ($r = 0.878$; $P < .001$; Figure 3). Most SCIs were located in white matter, with larger SCI volumes in white (median, 278 mm³; IQR, 125-772 mm³) compared with gray matter (median, 33 mm³; IQR, 3-146 mm³; $P < .001$). Children were most likely to have SCIs in the frontal lobes, followed by parietal, temporal, and occipital lobes (Table 2).

Silent cerebral infarcts occur in the region of lowest cerebral blood flow

The infarct density map was divided into regions of low (1%-6%), moderate (7%-12%), and high (13%-18%) infarct density. An independent cohort of 41 children with SCA and resting cerebral blood flow was used to evaluate cerebral blood flow within these 3 regions. Baseline characteristics are summarized in Table 1. Fourteen of the 41 children (34%) had SCIs with median infarct volume 314 mm³ (IQR, 158-844 mm³). Individual white matter cerebral blood flow was measured within each of the 3 regions. Cerebral blood flow was lowest in the region of highest infarct density ($P < .001$; Figure 4). Pairwise comparisons of white matter cerebral blood flow between the 3 infarct density tiers were significant after adjustment for multiple comparisons ($P < .05$). These data confirm that a nadir in resting cerebral blood flow may contribute to elevated and symmetric infarct densities in the border zone regions in pediatric SCA.

Infarct density maps for children with overt infarct or children with SCIs and recurrent infarcts

To compare brain regions commonly affected by SCIs with brain regions affected by overt infarct, children who were screened for the SIT Trial, but excluded because of having an overt infarct, and who had an MRI available for lesion delineation (n = 13) were included in a separate infarct density map (Table 1; Figure 5A). Similar to SCIs, overt infarcts were predominantly located within the border zone region (Figure 5B), but were larger in volume when compared with SCIs in the SIT Trial: infarct volumes were median 0.046% of total brain volume (IQR, 0.026%-0.421%) for overt vs 0.034% (IQR, 0.018%-0.092%) for silent ($P = .034$). Baseline and 3-year follow-up infarct density maps in children

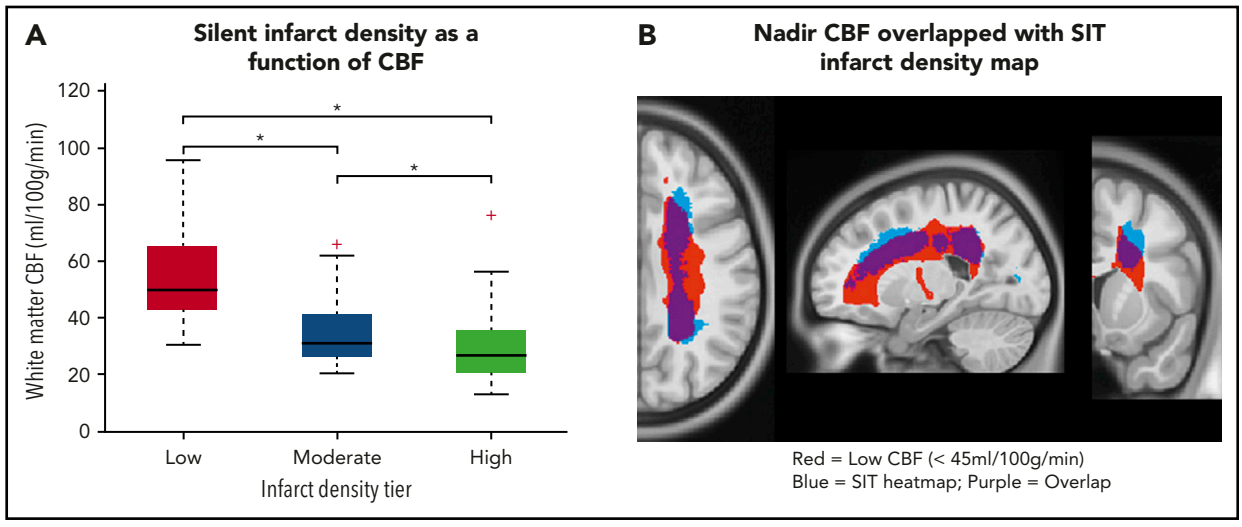

Figure 4. White matter cerebral blood flow is lowest in regions of highest infarct density. Resting cerebral blood flow maps from an independent cohort of children with SCA were aligned to the infarct density map of the SIT Trial participants. (A) Mean cerebral blood flow was measured within 3 regions of low, moderate, and high infarct density. White matter cerebral blood flow was lowest in the region of highest infarct density (Friedman Test, $P < .001$). *Pairwise tests for low- vs moderate-infarct-density, moderate- vs high-infarct-density, and low- vs high-infarct-density tiers, were significant after adjustment for multiple comparisons ($P < .05$). These data confirm that a nadir in resting cerebral blood flow may contribute to elevated and symmetric infarct densities in the border zone regions in pediatric SCA. (B) Nadir cerebral blood flow map (defined as average cerebral blood flow <45 mL/100 g/min) from the independent pediatric SCA cohort overlaid onto the infarct density map of the SIT Trial participants thresholded to include SCIs from 90% of the SIT Trial cohort. A high degree of overlap is found between nadir cerebral blood flow in the border zone region and regions of peak infarct density. CBF, cerebral blood flow.

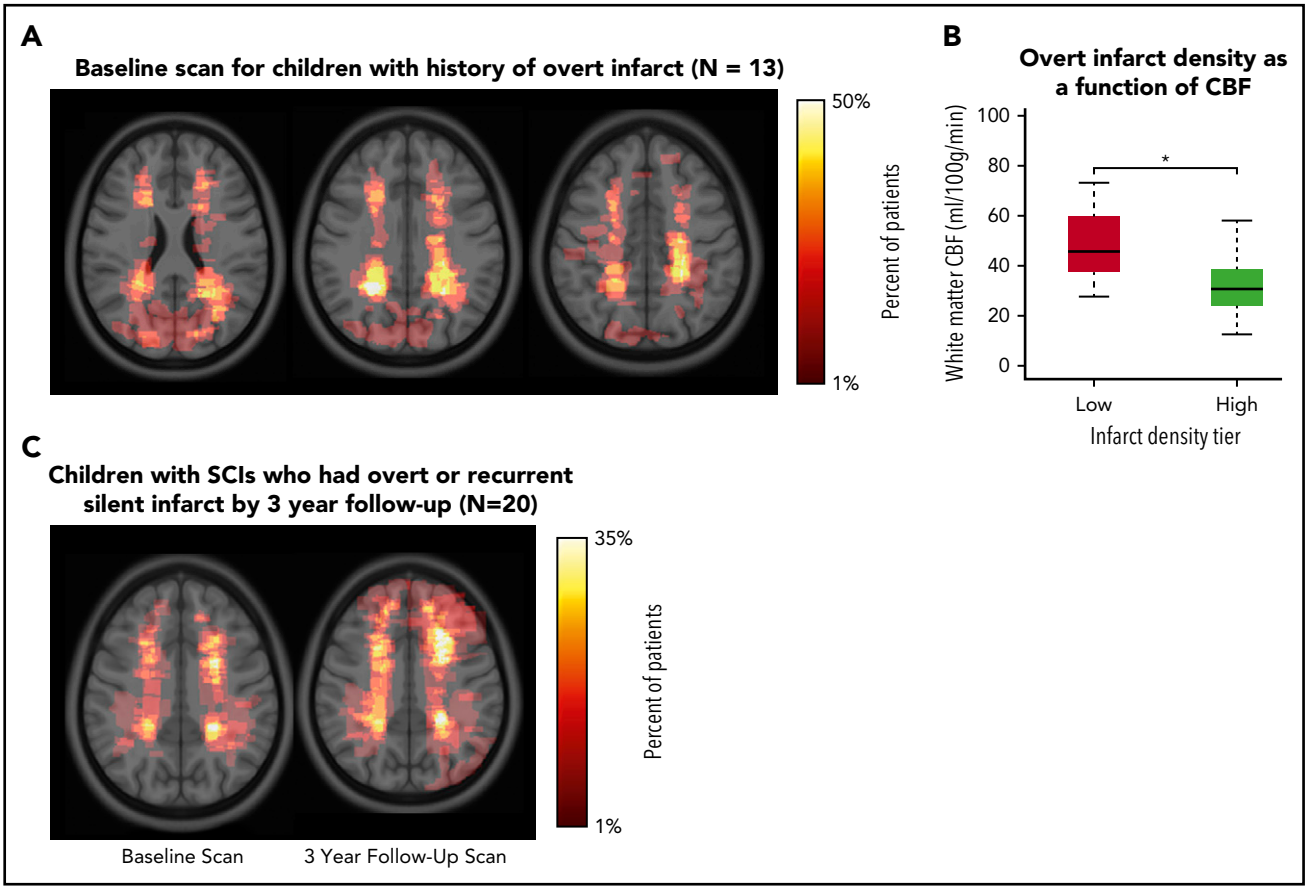

Figure 5. Infarct density maps in children with overt infarct and in children with SCIs who had overt infarct or recurrent silent infarcts by 3-year follow-up. (A) Infarct density map for children in the SIT Trial with SCIs, but excluded from adjudication as an SCI as a result of having an overt infarct (n = 13). Overt infarcts are predominantly located within the border zone region, however, were larger and extend into the gray matter. (B) Mean cerebral blood flow was measured within regions of low (1%-25%) and high (26%-50%) infarct density. *White matter cerebral blood flow was lower in the region of highest infarct density (Wilcoxon rank sum test, $P < .001$). Similar to finding low cerebral blood flow in region of high silent infarct density, these data are suggestive that a nadir in resting cerebral blood flow may contribute to the presence of overt infarcts. (C) Infarct density map for the subset of children in the SIT Trial with SCIs who had overt or recurrent silent infarcts by 3-year follow-up (n = 20). Baseline MRI is shown on left, and 3-year follow-up MRI is shown on right. The baseline MRI scan demonstrated significantly larger lesions than baseline lesions from the larger SIT Trial cohort. The influence of baseline infarct volume on infarct recurrence was evaluated using logistic regression models (Table 3). By 3-year follow-up, the infarct pattern demonstrated persistent regional vulnerability within the border zone territory, yet lesions were enlarged and extended into gray matter.

with SCIs (and no stroke history) who had overt or silent infarct at 3-year follow-up (n = 20) are shown in Figure 5C. For this subgroup of children with recurrent infarct, the baseline MRI scan demonstrated larger lesions compared with the baseline scan from children who did not have infarct recurrence: infarct volumes (percentage of total brain) were median 0.101% (IQR, 0.032%-0.618%) for those with recurrence vs 0.034% (IQR, 0.018%-0.089%) for those without recurrence ($P < .001$).

Imaging and clinical predictors of overt stroke or recurrent silent infarct

Logistic regression evaluated the effects of baseline imaging and clinical characteristics on incident overt stroke or recurrent SCIs. For prediction of overt stroke in the SIT Trial cohort (n = 286), baseline infarct volume as a percentage of total brain volume was independently associated with overt stroke in the multivariable logistic regression model (odds ratio, 9.20; $P = .001$; Table 3). The ratio of gray to white matter FLAIR lesion volume and percentage of lesion inside the 90% heat map were not predictive. Of clinical predictors, steady-state reticulocytes (odds ratio, 1.10; $P = .008$) independently predicted overt stroke (Table 3).

A second logistic regression model evaluated imaging and clinical predictors of overt stroke and recurrent silent infarct within the SIT randomized cohort only (n = 196). This smaller cohort had 2 unique assessments. First, the randomly allocated cohort permitted the assessment of the effect of regular blood transfusions on recurrent infarct. Second, the cohort allowed for the primary end point to include both incident overt stroke and recurrent SCI. Younger age, steady-state reticulocytes, parental report of recurrent headache, and randomization to observational care rather than transfusion were significant predictors of overt stroke and recurrent SCI at 3 years; whereas, baseline imaging predictors were not predictive (Table 3).

Discussion

Silent cerebral infarcts in children with SCA are common, progressive, and associated with cognitive morbidity.[4-8,31,32] We tested the hypothesis that the majority of SCIs would occur in the border zone region and the highest density of SCIs would occur in the region of lowest cerebral blood flow. In a large cohort of children with SCA and SCIs, we identified that the majority of SCIs were located within a common region in the deep white

Table 3. Imaging and clinical predictors of incident overt stroke and recurrent silent infarcts in children with sickle cell anemia and silent cerebral infarcts in the SIT Trial

	Odds ratio (95% confidence interval)	*P*
Prediction of incident overt stroke: non-randomized and randomized children (N = 286)		
Imaging predictors		
FLAIR lesion volume (% of brain)	9.20 (3.01-28.08)	.001
Gray to white matter FLAIR volume ratio	—	—
Percentage of lesion volume inside 90% heat map	—	—
Clinical predictors		
Age at registration, years	—	—
Steady-state reticulocytes (%)	1.10 (1.01-1.20)	.008
Parental report of recurrent headaches	—	—
Prediction of incident overt stroke and recurrent silent infarcts: randomized children only (N = 196)		
Imaging predictors		
FLAIR lesion volume (% of brain)	—	—
Gray to white matter FLAIR volume ratio	—	—
Percentage of lesion volume inside 90% heat map	—	—
Clinical predictors		
Age at randomization, years	0.72 (0.56-0.89)	.004
Steady-state reticulocytes (%)	1.10 (1.01-1.22)	.040
Parental report of recurrent headache	4.06 (1.43-12.85)	.011
Randomization to transfusion (vs observation)	0.30 (0.09-0.88)	.036

matter (Figure 2; Table 2). Further, by overlaying cerebral blood flow maps from an independent cohort of children with SCA, we demonstrated cerebral blood flow decreased as infarct density increased (Figure 4). These results are consistent with previous findings of stroke location in SCA showing that both SCIs fall within the white matter of the frontal and parietal lobes, and specifically within the border zone vascular distribution.[4,18,33] Our findings are unique, in that we show 90% of children have SCIs within a relatively small border zone region, measuring 5.6% of total brain volume, and they occur in the region of low blood flow.

After demonstrating the strong relationship between border zone cerebral blood flow and SCI density, we further investigated the group with overt infarcts (excluded after screening), as well as the group with recurrent SCIs in those with pre-existing SCI and followed up for approximately 3 years (clinical trial participants). Both subgroups demonstrated peak lesion density in the internal border zone, although baseline infarct volumes were larger (Figure 5). Despite a small cohort of overt infarcts (n = 13), we found a strong relationship between low resting cerebral blood flow and increased lesion density (Figure 5B). These preliminary data suggest that overt infarcts share a similar stroke mechanism to silent infarction with regard to border zone ischemic vulnerability. Given the small sample size of this cohort, the overt infarct density map does not exclude other stroke mechanisms. Children with SCA are at increased risk for stroke from several mechanisms, including embolic and hemorrhagic etiologies; however, our findings indicate border zone vulnerability is a common pattern, as found in SCIs. A recent study by Fields et al[33] demonstrated a region of elevated oxygen extraction fraction that overlapped with greatest infarct density within a cohort of children with SCA and SCIs. Within the elevated oxygen extraction fraction region, cerebral blood flow was low, likely representing the internal border zone. Elevated oxygen extraction fraction likely represents a compensatory response to inadequate cerebral oxygen delivery suggestive of chronic ischemia in the border zone region. Taken together, these data demonstrate the intrinsic vulnerability of the deep white matter in pediatric SCA, with the nadir in resting cerebral blood flow strongly influencing the risk for both silent and overt infarct to this region.

Presence of a SCI or prior overt stroke are known predictors of infarct recurrence[4,10,34]; however, imaging predictors of recurrence such as lesion volume have not been thoroughly evaluated in SCA. In our study, neither the ratio of gray to white matter SCI volume nor the percentage of lesion within the thresholded the infarct density map of the SIT Trial participants predicted infarct recurrence. Only FLAIR lesion volume, adjusted by brain volume, was predictive of overt stroke in the larger SIT Trial cohort, but this baseline variable was no longer predictive in the smaller randomized cohort when treatment assignment to observation vs transfusion was included and when the end point included both silent and overt infarct. These results suggest the possibility that baseline infarct volume is more predictive of overt infarct than recurrent silent infarct; however, further studies are needed. Studies of nonsickle cell adult cerebrovascular disease have shown that baseline lesion volume predicts recurrent ischemic stroke[35] and white matter disease progression.[36] Magnetic resonance angiography (MRA)-defined cerebral vasculopathy is an important risk factor for children with SCA and overt strokes receiving blood transfusion therapy[37]; however, MRA-defined intracranial vasculopathy is infrequent in children with SCA and SCIs who have normal or conditional TCD velocities, occurring in less than 2% of the SIT population who received MRA.[38]

Parental report of recurrent headaches predicted infarct recurrence in the randomized cohort of the SIT Trial. In a previous study, Dowling et al[39] found no association between presence of SCIs

and recurrent headaches; however, this was a cross-sectional study from the larger SIT Trial cohort, including a majority of the children screened with MRI (n = 872). In contrast, when children with SCIs in the SIT Trial were followed longitudinally, parental report of recurrent headaches was a significant predictor of recurrence. Although the longitudinal data suggest a temporal association between headache and infarct recurrence, a prospective study focused on assessment of headaches in children with SCA would be needed to confirm whether headache predicts infarct recurrence.

The major strengths of the study include that this was a planned ancillary study of the multicenter SIT Trial, with rigorous inclusion and exclusion criteria, and central adjudication of SCIs in a panel of neuroradiologists and neurologists. We believe our infarct density map is representative and accurate for SCI spatial prediction in children with SCA and normal or conditional TCD readings. Identification of SCIs in children with SCA is often in the setting of a SCI being singular and a small, minimum diameter of 3 mm, such that these lesions can be difficult to detect. As a result of the SCI density map presented here, neuroradiologists can have higher confidence that suspected lesions in the hotspots for SCI are indeed likely to be SCI.

Our study had inherent limitations. Our results are specific to children with SCIs and normal or conditional TCD velocities (<200 cm/s), a subgroup that represents the majority of children with SCIs. Our preliminary results also indicate that children with overt stroke have a similar border zone distribution as children with SCIs. We expect flow-limiting intracranial vasculopathy to have been rare in the SCI density population, given that 2%-6% of children with SCA and normal or conditional TCD velocities demonstrate intracranial vasculopathy.[14,38]

To identify the relationship between cerebral blood flow and SCI density, we used an independent cohort of children with SCA who had prospectively acquired cerebral blood flow imaging, one-third of whom had SCIs. The specifications of the non-SIT Trial cohort allowed a similar cohort to the SIT Trial (Table 1), including nontransfused children and excluding children with overt stroke, elevated TCD velocities, or intracranial vasculopathy. In addition, SCIs from this independent cohort were manually outlined and excluded from the analysis to prevent inclusion of dead, nonperfused tissue in the assessment of low cerebral blood flow. The observation that the lowest cerebral blood flow region shows striking overlap with the SCI and overt infarct lesion density maps suggests a region of vulnerability before accumulating SCIs and overt infarcts. Evaluating cerebral blood flow in the independent cohort of children with SCA and low SCI burden strengthens the generalizability of our findings for targeting therapeutic strategies to prevent SCI and overt strokes.

For the arterial spin labeling cerebral blood flow analysis, images were obtained using a postlabel delay of 1.0 seconds before the recommendation to use a postlabel delay of 1.5 seconds.[40] These recommendations were made for normal children, not for children with SCA, who have greatly elevated cerebral blood flow and reduced transit time relative to nonanemic children. Further, the current analysis assessed cerebral blood flow differences within an individual participant across regions of increasing infarct density; thus, although absolute cerebral blood flow could be overestimated, relative changes in cerebral blood flow are valid.

In a large multicenter population of children with SCA and normal or conditional TCD values, the majority of SCIs are symmetrically located in white matter of the internal border zone, where resting cerebral blood flow is at a nadir. The infarct density map provides a template for future studies evaluating novel imaging biomarkers predicting stroke risk in SCA, and will assist neuroradiologists in identifying SCIs within this established region. Collectively, our data provide the physiological basis for targeting primary and secondary infarct prevention therapies that augment cerebral blood flow in the internal border zone.

Acknowledgments

The authors acknowledge the families and the study participants from the SIT Trial that endured 3 magnetic resonance images, coupled with monthly blood transfusions for 3 years, 2 cognitive testing sessions, and multiple pediatric neurology and hematology evaluations to complete the SIT Trial. We also acknowledge the 3 neuroradiologists (Bob Mckinstry, William Ball, and Michael Kraut, who reviewed more than 1400 magnetic resonance imaging scans. A special thanks to Bob Mckinstry, who tirelessly identified the SCIs during the course of the trial and provided the groundwork for this manuscript.

This work was supported by the National Institutes of Health (NIH) National Heart, Lung, and Blood Institute (R01HL129241, A.L.F; K23HL136904 and K12HL087197, M.E.F.); NIH National Institute of Neurological Disorders and Stroke (5U01NS042804, 3U01NS042804, American Recovery Reinvestment ACT supplementary grant, M.R.D.; R01NS085419, R01NS084028, R01NS094692, R21AG05533301, J.-M.L.; R01NS082561 and P30NS098577, H.A.; K23NS099472, K.P.G.); Child Neurology Foundation (K.P.G.); Pediatric Critical Care and Trauma Scientist Development Program (K12 HD04734, K.P.G.); Washington University St. Louis, Clinical and Translational Science Award (UL1 TR000448, K.P.G., M.E.F.); and Vanderbilt University Medical Center, Clinical and Translational Science Award UL1TR000445 (M.R.D.).

Authorship

Contribution: A.L.F. and M.R.D. designed the experiment, analyzed and interpreted data, and prepared the manuscript; M.E.F. and K.P.G. collected and interpreted the data; D.K.R., S.F., M.M.B., and H.A. processed and analyzed the data; L.C.J., R.C.M., and J.-M.L. designed the experiment and analyzed and interpreted data; and all authors critically reviewed and approved the final version of the manuscript.

Conflict-of-interest disclosure: The authors declare no competing financial interests.

ORCID profiles: A.L.F., 0000-0003-0605-8943; K.P.G., 0000-0002-5518-3778; H.A., 0000-0001-6459-2269; L.C.J., 0000-0001-7240-0415; R.C.M., 0000-0003-3578-4899; J.-M.L., 0000-0002-3979-0906; M.R.D., 0000-0002-0574-1604.

Correspondence: Andria L. Ford, Department of Neurology, Washington University School of Medicine, 600 South Euclid Ave, Campus Box 8111, Saint Louis, MO 63110; e-mail: forda@wustl.edu.

Footnotes

Submitted 8 April 2018; accepted 17 July 2018. Prepublished online as *Blood* First Edition paper, 30 July 2018; DOI 10.1182/blood-2018-04-841247.

There is a *Blood* Commentary on this article in this issue.

The publication costs of this article were defrayed in part by page charge payment. Therefore, and solely to indicate this fact, this article is hereby marked "advertisement" in accordance with 18 USC section 1734.

REFERENCES

1. DeBaun MR, Gordon M, McKinstry RC, et al. Controlled trial of transfusions for silent cerebral infarcts in sickle cell anemia. *N Engl J Med*. 2014;371(8):699-710.
2. Bernaudin F, Verlhac S, Arnaud C, et al. Impact of early transcranial Doppler screening and intensive therapy on cerebral vasculopathy outcome in a newborn sickle cell anemia cohort. *Blood*. 2011;117(4):1130-1140.
3. Kassim AA, Pruthi S, Day M, et al. Silent cerebral infarcts and cerebral aneurysms are prevalent in adults with sickle cell anemia. *Blood*. 2016;127(16):2038-2040.
4. Pegelow CH, Macklin EA, Moser FG, et al. Longitudinal changes in brain magnetic resonance imaging findings in children with sickle cell disease. *Blood*. 2002;99(8):3014-3018.
5. Schatz J, Brown RT, Pascual JM, Hsu L, DeBaun MR. Poor school and cognitive functioning with silent cerebral infarcts and sickle cell disease. *Neurology*. 2001;56(8): 1109-1111.
6. Armstrong FD, Thompson RJ Jr, Wang W, et al; Neuropsychology Committee of the Cooperative Study of Sickle Cell Disease. Cognitive functioning and brain magnetic resonance imaging in children with sickle Cell disease. *Pediatrics*. 1996;97(6 Pt 1):864-870.
7. DeBaun MR, Schatz J, Siegel MJ, et al. Cognitive screening examinations for silent cerebral infarcts in sickle cell disease. *Neurology*. 1998;50(6):1678-1682.
8. Bernaudin F, Verlhac S, Fréard F, et al. Multicenter prospective study of children with sickle cell disease: radiographic and psychometric correlation. *J Child Neurol*. 2000;15(5): 333-343.
9. DeBaun MR, Sarnaik SA, Rodeghier MJ, et al. Associated risk factors for silent cerebral infarcts in sickle cell anemia: low baseline hemoglobin, sex, and relative high systolic blood pressure. *Blood*. 2012;119(16):3684-3690.
10. Scothorn DJ, Price C, Schwartz D, et al. Risk of recurrent stroke in children with sickle cell disease receiving blood transfusion therapy for at least five years after initial stroke. *J Pediatr*. 2002;140(3):348-354.
11. Bernaudin F, Verlhac S, Arnaud C, et al. Chronic and acute anemia and extracranial internal carotid stenosis are risk factors for silent cerebral infarcts in sickle cell anemia. *Blood*. 2015;125(10):1653-1661.
12. Dowling MM, Quinn CT, Plumb P, et al. Acute silent cerebral ischemia and infarction during acute anemia in children with and without sickle cell disease. *Blood*. 2012;120(19): 3891-3897.
13. Thangarajh M, Yang G, Fuchs D, et al. Magnetic resonance angiography-defined intracranial vasculopathy is associated with silent cerebral infarcts and glucose-6-phosphate dehydrogenase mutation in children with sickle cell anaemia. *Br J Haematol*. 2012;159(3):352-359.
14. Arkuszewski M, Krejza J, Chen R, et al. Sickle cell anemia: intracranial stenosis and silent cerebral infarcts in children with low risk of stroke. *Adv Med Sci*. 2014;59(1):108-113.
15. Baldeweg T, Hogan AM, Saunders DE, et al. Detecting white matter injury in sickle cell disease using voxel-based morphometry. *Ann Neurol*. 2006;59(4):662-672.
16. Balci A, Karazincir S, Beyoglu Y, et al. Quantitative brain diffusion-tensor MRI findings in patients with sickle cell disease. *AJR Am J Roentgenol*. 2012;198(5):1167-1174.
17. Rothman SM, Fulling KH, Nelson JS. Sickle cell anemia and central nervous system infarction: a neuropathological study. *Ann Neurol*. 1986; 20(6):684-690.
18. Guilliams KP, Fields ME, Ragan DK, et al. Large-vessel vasculopathy in children with sickle cell disease: a magnetic resonance imaging study of infarct topography and focal atrophy. *Pediatr Neurol*. 2017;69:49-57.
19. Casella JF, King AA, Barton B, et al. Design of the silent cerebral infarct transfusion (SIT) trial. *Pediatr Hematol Oncol*. 2010;27(2):69-89.
20. Jenkinson M, Bannister P, Brady M, Smith S. Improved optimization for the robust and accurate linear registration and motion correction of brain images. *Neuroimage*. 2002; 17(2):825-841.
21. Jenkinson M, Smith S. A global optimisation method for robust affine registration of brain images. *Med Image Anal*. 2001;5(2):143-156.
22. Bazin PL, Cuzzocreo JL, Yassa MA, et al. Volumetric neuroimage analysis extensions for the MIPAV software package. *J Neurosci Methods*. 2007;165(1):111-121.
23. Fonov V, Evans AC, Botteron K, Almli CR, McKinstry RC, Collins DL; Brain Development Cooperative Group. Unbiased average age-appropriate atlases for pediatric studies. *Neuroimage*. 2011;54(1):313-327.
24. Klein A, Andersson J, Ardekani BA, et al. Evaluation of 14 nonlinear deformation algorithms applied to human brain MRI registration. *Neuroimage*. 2009;46(3):786-802.
25. Zhang Y, Brady M, Smith S. Segmentation of brain MR images through a hidden Markov random field model and the expectation-maximization algorithm. *IEEE Trans Med Imaging*. 2001;20(1):45-57.
26. Mazziotta J, Toga A, Evans A, et al. A probabilistic atlas and reference system for the human brain: International Consortium for Brain Mapping (ICBM). *Philos Trans R Soc Lond B Biol Sci*. 2001;356(1412):1293-1322.
27. Wu WC, Fernández-Seara M, Detre JA, Wehrli FW, Wang J. A theoretical and experimental investigation of the tagging efficiency of pseudocontinuous arterial spin labeling. *Magn Reson Med*. 2007;58(5):1020-1027.
28. Jain V, Duda J, Avants B, et al. Longitudinal reproducibility and accuracy of pseudo-continuous arterial spin-labeled perfusion MR imaging in typically developing children. *Radiology*. 2012;263(2):527-536.
29. Biagi L, Abbruzzese A, Bianchi MC, Alsop DC, Del Guerra A, Tosetti M. Age dependence of cerebral perfusion assessed by magnetic resonance continuous arterial spin labeling. *J Magn Reson Imaging*. 2007;25(4):696-702.
30. Hales PW, Kirkham FJ, Clark CA. A general model to calculate the spin-lattice (T1) relaxation time of blood, accounting for haematocrit, oxygen saturation and magnetic field strength. *J Cereb Blood Flow Metab*. 2016;36(2):370-374.
31. DeBaun MR, Armstrong FD, McKinstry RC, Ware RE, Vichinsky E, Kirkham FJ. Silent cerebral infarcts: a review on a prevalent and progressive cause of neurologic injury in sickle cell anemia. *Blood*. 2012;119(20):4587-4596.
32. Kassim AA, DeBaun MR. The case for and against initiating either hydroxyurea therapy, blood transfusion therapy or hematopoietic stem cell transplant in asymptomatic children with sickle cell disease. *Expert Opin Pharmacother*. 2014;15(3):325-336.
33. Fields ME, Guilliams KP, Ragan DK, et al. Regional oxygen extraction predicts border zone vulnerability to stroke in sickle cell disease. *Neurology*. 2018;90(13):e1134-e1142.
34. Miller ST, Macklin EA, Pegelow CH, et al; Cooperative Study of Sickle Cell Disease. Silent infarction as a risk factor for overt stroke in children with sickle cell anemia: a report from the Cooperative Study of Sickle Cell Disease. *J Pediatr*. 2001;139(3):385-390.
35. Asdaghi N, Hameed B, Saini M, Jeerakathil T, Emery D, Butcher K. Acute perfusion and diffusion abnormalities predict early new MRI lesions 1 week after minor stroke and transient ischemic attack. *Stroke*. 2011;42(8):2191-2195.
36. van Dijk EJ, Prins ND, Vrooman HA, Hofman A, Koudstaal PJ, Breteler MM. Progression of cerebral small vessel disease in relation to risk factors and cognitive consequences: Rotterdam Scan study. *Stroke*. 2008;39(10):2712-2719.
37. Hulbert ML, McKinstry RC, Lacey JL, et al. Silent cerebral infarcts occur despite regular blood transfusion therapy after first strokes in children with sickle cell disease. *Blood*. 2011; 117(3):772-779.
38. Choudhury NA, DeBaun MR, Ponisio MR, et al. Intracranial vasculopathy and infarct recurrence in children with sickle cell anaemia, silent cerebral infarcts and normal transcranial Doppler velocities [published online ahead of print 26 October 2017]. *Br J Haematol*. doi:org/10.1111/bjh.14979.
39. Dowling MM, Noetzel MJ, Rodeghier MJ, et al. Headache and migraine in children with sickle cell disease are associated with lower hemoglobin and higher pain event rates but not silent cerebral infarction. *J Pediatr*. 2014; 164(5):1175-1180.
40. Alsop DC, Detre JA, Golay X, et al. Recommended implementation of arterial spin-labeled perfusion MRI for clinical applications: A consensus of the ISMRM perfusion study group and the European consortium for ASL in dementia. *Magn Reson Med*. 2015; 73(1):102-116.